

ENERGYMOGEN: Compositional Human Motion Generation with Energy-Based Diffusion Model in Latent Space

Jianrong Zhang¹, Hehe Fan^{2,†}, Yi Yang²

[†]Corresponding author

¹ReLER, AAIL, University of Technology Sydney ²CCAI, Zhejiang University

<https://jiro-zhang.github.io/EnergyMoGen/>

Abstract

Diffusion models, particularly latent diffusion models, have demonstrated remarkable success in text-driven human motion generation. However, it remains challenging for latent diffusion models to effectively compose multiple semantic concepts into a single, coherent motion sequence. To address this issue, we propose EnergyMoGen, which includes two spectrums of Energy-Based Models: ❶ We interpret the diffusion model as a latent-aware energy-based model that generates motions by composing a set of diffusion models in latent space; ❷ We introduce a semantic-aware energy model based on cross-attention, which enables semantic composition and adaptive gradient descent for text embeddings. To overcome the challenges of semantic inconsistency and motion distortion across these two spectrums, we introduce Synergistic Energy Fusion. This design allows the motion latent diffusion model to synthesize high-quality, complex motions by combining multiple energy terms corresponding to textual descriptions. Experiments show that our approach outperforms existing state-of-the-art models on various motion generation tasks, including text-to-motion generation, compositional motion generation, and multi-concept motion generation. Additionally, we demonstrate that our method can be used to extend motion datasets and improve the text-to-motion task.

1. Introduction

Composition of complex ideas out of simple ones.
– John Locke (1632 - 1704) [4]

Generating human motions that are both visually appealing and physically plausible is a longstanding goal in computer animation. Recently, the remarkable success of diffusion models [24, 52, 55] stimulates the emergence of diffusion-based solutions for generating human motion [58, 60, 70, 71] from a single text prompt.

Humans are masters of motion composition. For example, with the mind of “raising both arms” and “walking forward”, we can blend these simple concepts to perform complex motions simultaneously based on our experiences. To achieve this capability, past efforts, such as PriorMDM [53] and GMD [31], have made significant strides in temporal [2] and spatial [3] human motion compositions using pre-trained skeleton-based diffusion models. These models operate directly on skeletons, thus enabling precise control over joint feature distributions to generate realistic motions from multiple textual descriptions.

In this work, we are interested in the motion latent diffusion model [52, 64], which is another important formulation of diffusion models operating in continuous latent space. However, such models are not feasible for composing motion through algorithms proposed in skeleton-based diffusion models. As latent diffusion models map motions of varying lengths into a fixed number of tokens, the following issues naturally arise: *i*) Using the fixed number of tokens to represent motions can not support per-frame composition; *ii*) Lack of explicit correspondence between the latent feature and skeleton.

Tackling these two issues can offer valuable insights into compositional motion generation algorithms and motivate us to reconsider this task from an energy view. The idea of “energy” is intrinsic to Energy-Based Models (EBMs) [34]. Research on EBMs has a long history, yet it gets overlooked nowadays in human motion generation. The energy function defines a potential field to shape the energy surface by assigning low energies to desired configurations and high energies to other configurations [74]. With this perspective [7–9, 11, 43], we delve into two spectrums of EBMs for compositional motion generation: ❶ *latent-aware* and ❷ *semantic-aware*. By formulating the generative process of latent diffusion models as an energy combination problem, we can compose complex motions from simple components through two compositional operations: **conjunction** and **negation** (Figure 1 (a), (b), (c), more visual results are provided in § 5.4 and on the [project page](#)).

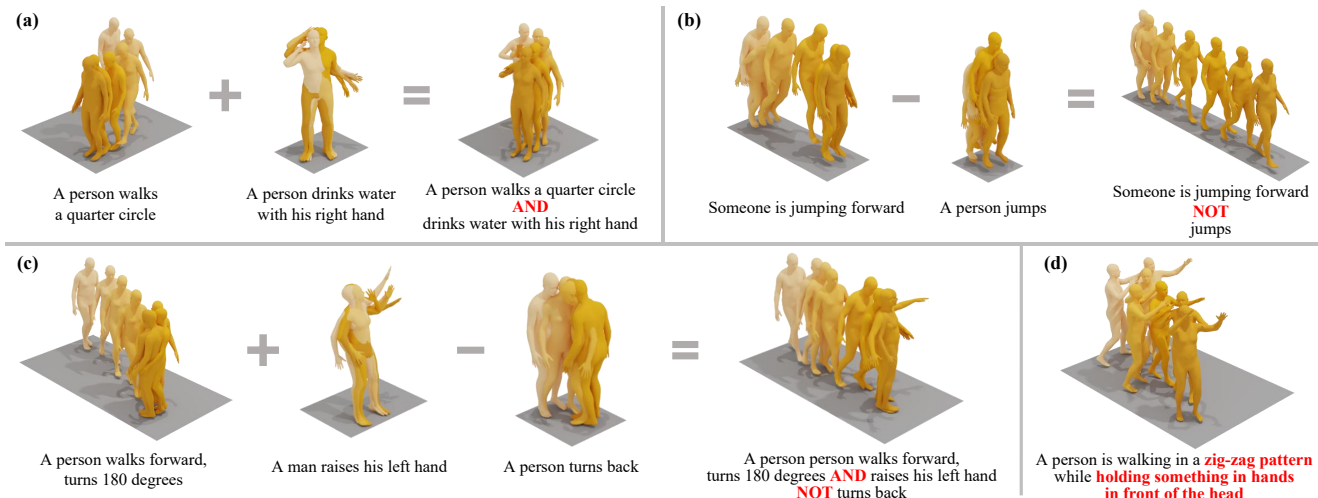


Figure 1. **Compositional motion generation.** Our approach is able to compose complex motions from simple concepts in settings of (a) concept conjunction, (b) concept negation, (c) compositional motion generation with conjunction and negation, and (d) multi-concept motion generation (a form of compositional generation).

Concretely, we propose ENERGYMOGEN, a compositional motion generation framework that incorporates cross-attention within the denoising autoencoder. We view latent diffusion models as latent-aware EBMs and illustrate the connection between them. Leveraging classifier-free guidance [23], we are able to compose motions by implicitly combining energy terms (*i.e.*, latent distributions) of multiple diffusion models. In addition, we introduce a semantic-aware EBM based on the cross-attention mechanism that supports a semantic-aware energy mixture for motion composition. Meanwhile, this energy-based cross-attention enables the adaptive updating of text embeddings by calculating the gradient of the energy function [43], which facilitates the generation of multi-concept motions from a single textual description (Figure 1 (d)).

Driven by our exploration, we insightfully find there are two critical limitations of the two spectrums in motion composition: **First**, the latent-aware composition has the problem of text misalignment. **Second**, the semantic-aware composition suffers from foot sliding and motion jitter. To alleviate these issues, we propose a Synergistic Energy Fusion (SEF) strategy by integrating distributions of latent-aware composition, semantic-aware composition, and multi-concept generation.

Taking these innovations together, ENERGYMOGEN becomes a general and flexible framework for compositional motion generation (our approach can easily generalize to skeleton-based diffusion models, and the results are provided in Section B of the appendix). Empirically, we show impressive results on three datasets across three tasks, *i.e.*, HumanML3D [19] and KIT-ML [49] for text-to-motion generation task (§ 5.3), MTT [47] for compositional motion generation and multi-concept motion generation tasks

(§ 5.4). We conduct comprehensive experiments for in-depth dissection (§ 5.5) to reveal the effectiveness of ENERGYMOGEN. Additionally, we introduce a CompML dataset (§ 5.1) comprising 5000 compositionally generated motion sequences with textual descriptions. We show that the model’s performance can be improved via training on composed motions (§ 5.5). We hope these experiments and conclusions will contribute to future developments.

2. Preliminaries: Energy-Based Models

In contrast to explicitly modeling the data distribution, Energy-based models (EBMs) [34, 74] implicitly define the underlying probability density of the distribution through an energy function. For a data sample \mathbf{X} , the probability density can be defined via the Boltzmann distribution:

$$p_{\theta}(\mathbf{X}) = \frac{\exp(-E_{\theta}(\mathbf{X}))}{Z(\theta)}, \quad (1)$$

where $Z(\theta) = \int \exp(-E_{\theta}(\mathbf{X}))d\mathbf{X}$ is the partition function, and $E_{\theta}(\mathbf{X})$ denotes the energy function, often parameterized as a neural network. However, EBMs struggle to calculate the partition function, making training challenging. Recent endeavors have been devoted to optimizing the Markov Chain Monte Carlo (MCMC) methods via *e.g.*, Langevin dynamics [7, 11], contrastive divergence [9], and score-based models [27, 56].

In addition, the modern Hopfield networks [25, 50] interpret the self-attention as EBMs. [50] introduces an energy function $E(\mathbf{X}, \xi) = -\alpha^{-1} \log \sum_{i=1}^N \exp(\alpha(\mathbf{X}^{\top} \xi)_i) + \frac{1}{2} \xi^{\top} \xi$ and a update rule $\xi_{new} = \xi - \gamma(\xi - \mathbf{X} \text{softmax}(\alpha \mathbf{X}^{\top} \xi))$, where the data sample \mathbf{X} consists of N stored patterns (key) $\mathbf{x}_i \in \mathbb{R}^d$, $\xi \in \mathbb{R}^d$ denotes

the state vector (query), and γ is the update step size. By linearly projecting \mathbf{X} and ξ into Query (\mathbf{Q}), Key(\mathbf{K}), and Value(\mathbf{V}), the attention mechanism can be understood as the energy update $\mathbf{Q}_{new} = \text{softmax}(\alpha \mathbf{Q} \mathbf{K}) \mathbf{V}$, when $\gamma = 1$ and $\alpha = 1/\sqrt{d}$. On this basis, Park *et al.* [43] extends the theory to cross-attention to handle several tasks, *e.g.*, image editing and inpainting.

3. Method

In this section, we introduce our approach, ENERGYMOGEN. We first present the architecture and formulations of the diffusion model in § 3.1. Next, we discuss the connection between diffusion models and energy-based models, as well as how to compose motions from several concepts through Synergistic Energy Fusion (SEF) in § 3.2. The overall framework is illustrated in Figure 2.

3.1. ENERGYMOGEN for Motion Generation

We build the architecture of ENERGYMOGEN upon motion latent diffusion model [64], which comprises two transformer-based modules: Motion Variational Autoencoder and Motion Latent Diffusion (in Figure 2 (a), (b)).

Motion Variational Autoencoder. Given a motion sequence $\mathbf{X} = [\mathbf{x}^1, \mathbf{x}^2, \dots, \mathbf{x}^L]$ with $x^l \in \mathbb{R}^{d_m}$, where L and d_m are the length and dimension of motion, we aim to reconstruct the motion via a Variational Autoencoder (VAE). Denoting the encoder and decoder as \mathcal{E} and \mathcal{D} , the encoded latent $z = \mathcal{E}(\mathbf{X})$, can be sampled from the distribution parameters (mean and variance) using reparameterization trick [32], where $z \in \mathbb{R}^{N \times d}$, N and d are the number of vectors and latent dimensions, respectively. With the reconstructed motion $\hat{\mathbf{X}} = \mathcal{D}(z)$, the VAE is trained to minimize the L1 smooth loss [68] for reconstruction and Kullback-Leibler (KL) divergence between the encoder distribution and normal distribution.

Motion Latent Diffusion with Energy-Based Cross Attention. Given the encoded motion latent z , a diffusion process aims to model a distribution of $q(z_t|z_{t-1}) = \mathcal{N}(z_t; \sqrt{1 - \beta_t} z_{t-1}, \beta_t I)$ to obtain a noisy latent z_t , where $t \in T$ is the timestep and $0 < \beta \leq 1$.

A denoising autoencoder ϵ_θ is employed to predict the underlying score of the distribution $\epsilon \sim \mathcal{N}(0, 1)$ based on the text embedding $\mathbf{c} \in \mathbb{R}^{N^t \times d}$. To optimize ϵ_θ , we minimize the standard optimization goal, *i.e.*, Mean Square Error (MSE), which can be formulated as follows:

$$\mathbb{E}_{z, \mathbf{c}, \epsilon, t} \left[\|\epsilon - \epsilon_\theta(z_t, t, \mathbf{c})\|_2^2 \right]. \quad (2)$$

Building upon the architecture in MLD [64], we propose to employ cross-attention to incorporate text embeddings and motion latent features. In light of recent endorsers on energy-based attention mechanism [25, 50], we interpret the cross-attention as an energy-based operation to facilitate

multi-concept motion generation. Specifically, \mathbf{K} and \mathbf{V} in cross attention is computed as $\mathbf{K} = \mathbf{c} W_{\mathbf{K}}$ and $\mathbf{V} = \mathbf{c} W_{\mathbf{V}}$, where $W_{\mathbf{K}}, W_{\mathbf{V}} \in \mathbb{R}^{d \times d}$. To alleviate the impact of misalignment in multi-concept text embeddings, we focus on refining \mathbf{c} through adaptive gradient descent (AGD) based on MAP estimation with $p(\mathbf{K}|\mathbf{Q}) \propto p(\mathbf{Q}|\mathbf{K})p(\mathbf{K})$. We introduce two energy functions, $E(\mathbf{K})$ and $E(\mathbf{Q}|\mathbf{K})$, done in the prior work [43]. Then, the gradient of log distribution can be written as:

$$\begin{aligned} \nabla_{\mathbf{K}} \log p(\mathbf{K}|\mathbf{Q}) &= \nabla_{\mathbf{K}} E(\mathbf{K}) - \nabla_{\mathbf{K}} E(\mathbf{Q}|\mathbf{K}) \\ &= \underbrace{[\text{SFM}(\alpha \mathbf{K} \mathbf{Q} \mathbf{Q}^\top) \mathbf{Q}]}_{\text{Attention}} - \underbrace{\mathcal{M}(\text{SFM}(\mathbf{K}')) \mathbf{K}}_{\text{Regularization}} W_{\mathbf{K}}, \end{aligned} \quad (3)$$

where SFM and \mathcal{M} are softmax and diagonalization operator, respectively, $\mathbf{K}' = \frac{1}{2} \sum_{i=1}^{N^t} k_i k_i^\top$, k_i denotes the i -th row of \mathbf{K} . Finally, \mathbf{c} is refined with the step size γ :

$$\hat{\mathbf{c}} = \mathbf{c} + \gamma \nabla_{\mathbf{K}} \log p(\mathbf{K}|\mathbf{Q}). \quad (4)$$

By doing so, we can induce the network to focus on the low-energy regions that are relevant to semantics within a multi-concept text. More detailed theoretical analysis can be found in [43].

3.2. Compositional Human Motion Generation with Energy-Based Diffusion Models

With the pre-trained latent motion diffusion model available, we can compose motions by integrating energy functions (Figure 2 (c)) in the latent space.

Bridging Diffusion Models and Energy-Based Models. During inference, the diffusion model aims to predict the distribution of $p(z_{t-1}|z_t)$ (or $q(z_{t-1}|z_t, z_0)$) to denoise z_t to z_{t-1} . By leveraging the Gaussian distribution, we define $p(z_{t-1}|z_t) := \mathcal{N}(z_{t-1}; \mu_\theta(z_t, t), \tilde{\beta}_t I)$. With $\mu_\theta(\cdot)$ approximated by $z_t - \epsilon_\theta(z_t, \mathbf{c}, t)$ for small β_t , the denoising step can be written as:

$$z_{t-1} = z_t - \epsilon_\theta(z_t, \mathbf{c}, t) + \mathcal{N}(0, \tilde{\beta}_t I). \quad (5)$$

In Energy-Based Models (EBMs), the Langevin Dynamics-based MCMC sampling is one of the most popular strategies for the generative process. According to [7, 8, 38, 61], each gradient descent step in the sampling process is defined as

$$z_{t-1} = z_t - \eta \nabla_z E_\theta(z_t, \mathbf{c}) + \mathcal{N}(0, \tilde{\beta}_t I), \quad (6)$$

which is similar to Equation 5. By representing the energy function $E_\theta(z_t, \mathbf{c})$ using the denoising autoencoder ϵ_θ , diffusion models can be interpreted as EBMs under the gradient descent step $\eta = 1$, enabling compositional motion generation via composing a set of diffusion models.

Compositional Motion Generation. Our goal is to synthesize motions from a set of concepts $\mathbb{C} = \{\mathbf{c}_i\}_{i=1}^n$ encoded

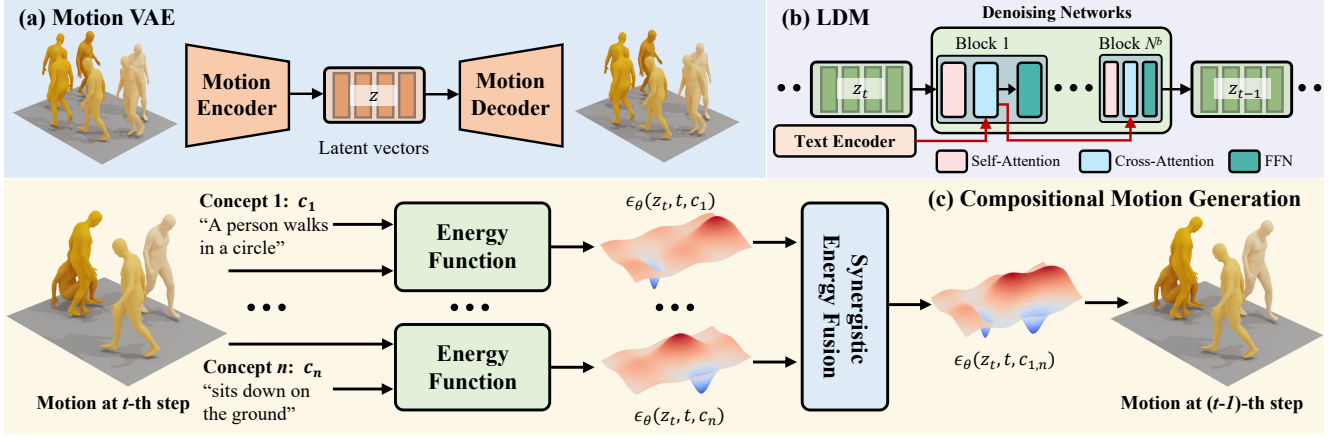


Figure 2. **Overview of ENERGYMOGEN.** (a) Motion Variational Autoencoder (VAE) maps 3D human motion into N latent vectors. (b) We use cross-attention-based transformers as the denoising network in the Latent Diffusion Model (LDM). N^b is the number of transformer layers. Cross-attention can be interpreted as an energy operation that facilitates multi-concept motion generation (Equation 3, 4). (c) We explore two spectrums of energy-based models and propose combining them with Synergistic Energy Fusion (SEF). The energy function can be either a denoising network (latent-aware) or a cross-attention (semantic-aware).

by the text encoder. We introduce compositional operators **conjunction** and **negation**. The former seeks to generate motion incorporating all concepts, while the latter proposes the exclusion of certain factors. We use an energy function to model individual concepts c_i and assemble them for motion composition. To achieve this, we explore two spectrums of EBMs: ① *latent-aware* and ② *semantic-aware*.

① For the latent-aware energy-based diffusion model, the probability distribution of conjunction is defined as $p(z|c_1, \dots, c_n) \propto p(z) \prod_{i=1}^n p(z|c_i)/p(z)$. Interpret $p(z|c_i)$ and $p(z)$ as conditional and unconditional distributions, respectively, we can easily connect $p(z|c_1, \dots, c_n)$ to classifier-free guidance [23], and the compositional sampling process can be factorized as:

$$\epsilon_{\theta}^l(z_t, t, \mathbb{C}) = \epsilon_{\theta}(z_t, t) + \sum_{i=1}^n w_i^l (\epsilon_{\theta}(z_t, t, c_i) - \epsilon_{\theta}(z_t, t)), \quad (7)$$

where w_i^l denotes the weight for i -th concept. Similarly, we follow [8, 38] to define the probability distribution of negation as $p(z|c_i, \text{not } c_j) \sim \frac{p(z)p(c_i|z)}{p(c_j|z)}$. Naturally, the composed distribution can be formulated as:

$$\epsilon_{\theta}^l(z_t, t, \mathbb{C}) = \epsilon_{\theta}(z_t, t) + w^l (\epsilon_{\theta}(z_t, t, c_i) - \epsilon_{\theta}(z_t, t, c_j)). \quad (8)$$

Through Equation 7 and Equation 8, we can generate compositional motions by manipulating latent vectors of pre-trained motion latent diffusion models.

② As discussed in § 3.1, cross-attention can be interpreted as an energy-based operation. We utilize this idea to introduce a semantic-aware EBM. Specifically, $\mathbb{Z}' = \{z'_i\}_{i=1}^n$ is a set of features derived from a cross-attention layer in ϵ_{θ} , that corresponds to concepts \mathbb{C} . Due to these

output features are unnormalized probability distributions, we compose them by performing a weighted average:

$$\hat{z}' = \frac{1}{\sum_{i=1}^n w_i^s} \sum_{i=1}^n (w_i^s z'_i), \quad (9)$$

w^s is a hyper-parameter to balance various concepts. $w^s > 0$ indicates a conjunction operation, while $w^s < 0$ suggests a negation operation. We consistently apply this combination across all cross-attention layers, obtaining the output distribution of $\epsilon_{\theta}^s(z_t, t, \mathbb{C})$.

Synergistic Energy Fusion. We empirically (§ 5.5) find that directly employing ① for compositional motion generation leads to semantic misalignment, while ② suffers from motion distortion (*e.g.*, foot slides and motion jitter). We propose Synergistic Energy Fusion (SEF) to mitigate these limitations. Given the concepts set \mathbb{C} and a text embedding $c_{1,n}$ of a single textual description with all concepts in \mathbb{C} . At the t -th step of the reverse process, we fuse distributions from ①, ②, and the single text with multiple concepts as follows:

$$\hat{\epsilon}_{\theta}(z_t, t, \mathbb{C}, c_{1,n}) = \lambda_l \epsilon_{\theta}^l(z_t, t, \mathbb{C}) + \lambda_s \epsilon_{\theta}^s(z_t, t, \mathbb{C}) + \lambda_m \epsilon_{\theta}(z_t, t, c_{1,n}), \quad (10)$$

where λ_l , λ_s and λ_m are hyper-parameters with $\lambda_l + \lambda_s + \lambda_m = 1$, $\hat{\epsilon}_{\theta}(\cdot)$ is the final score for the next reverse process.

4. Related Works

Text-driven Motion Generation. Text-driven motion generation, a rapidly evolving field, aims to bridge the gap between natural language descriptions and human motion.

Methods	R-Precision \uparrow			FID \downarrow	MM-Dist \downarrow	Diversity \rightarrow	MModality \uparrow
	Top-1	Top-2	Top-3				
Real motion	0.511 \pm .003	0.703 \pm .003	0.797 \pm .002	0.002 \pm .000	2.974 \pm .008	9.503 \pm .065	-
MDM [58]	0.418 \pm .005	0.604 \pm .001	0.707 \pm .004	0.489 \pm .025	3.630 \pm .023	9.450 \pm .066	2.870 \pm 1.11
MotionDiffuse [69]	0.491 \pm .001	0.681 \pm .001	0.782 \pm .001	0.630 \pm .001	3.113 \pm .001	9.410 \pm .049	1.553 \pm .042
M2DM [33]	0.497 \pm .003	0.682 \pm .002	0.763 \pm .003	0.352 \pm .005	3.134 \pm .010	9.926 \pm .073	3.587 \pm .072
Fg-T2M [60]	0.492 \pm .002	0.683 \pm .003	0.783 \pm .002	0.243 \pm .019	3.109 \pm .007	9.278 \pm .072	1.614 \pm .049
ReMoDiffusion [70]	0.510 \pm .005	0.698 \pm .006	<u>0.795</u> \pm .004	0.103 \pm .004	2.974 \pm .016	9.018 \pm .075	1.795 \pm .043
FineMoGen [71]	0.504 \pm .002	0.690 \pm .002	0.784 \pm .004	0.151 \pm .008	2.998 \pm .008	9.263 \pm .094	<u>2.696</u> \pm .079
MLD* [64]	0.481 \pm .003	0.673 \pm .003	0.772 \pm .002	0.473 \pm .013	3.196 \pm .010	9.724 \pm .082	2.413 \pm .079
GUESS* [13]	0.503 \pm .003	0.688 \pm .002	0.787 \pm .002	<u>0.109</u> \pm .007	3.006 \pm .007	9.826 \pm .104	2.430 \pm .100
MotionMamba* [73]	0.502 \pm .003	0.693 \pm .002	0.792 \pm .002	0.281 \pm .009	3.060 \pm .058	9.871 \pm .084	2.294 \pm .058
ENERGYMOGEN*	<u>0.523</u> \pm .003	<u>0.715</u> \pm .002	0.815 \pm .002	0.188 \pm .006	2.915 \pm .007	9.488 \pm .099	2.205 \pm 0.041
ENERGYMOGEN (CompML)*	0.526 \pm .003	0.718 \pm .003	0.815 \pm .002	0.176 \pm .006	<u>2.931</u> \pm .007	9.500 \pm .091	2.270 \pm 0.057

Table 1. **Comparison with the state-of-the-art diffusion models on the HumanML3D [19] test set.** We repeat the evaluation 20 times for each metric and report the average with a 95% confidence interval. Bold and underlined indicate the best and second-best results. Methods based on the latent diffusion model are marked with *.

Earlier works heavily rely on building a text-motion joint latent space [1, 16, 57]. However, due to their reliance on autoencoders, these methods are limited in producing high-quality and diverse motions. To address these limitations, various studies have explored VAE-based methods [2, 3, 19, 44–46] to sample motions from Gaussian distribution. Recently, TM2T [20] and T2M-GPT [68] have made significant progress by projecting human motions into discrete representations via Vector Quantized Variational AutoEncoders (VQ-VAE). On these bases, some studies focus on optimizing VQ-VAE [21, 40, 75], combining with large language models [28, 72], and exploring the mask language modeling strategy [48].

Diffusion models also show promising results in text-to-motion generation. Existing diffusion-based methods can be categorized into two groups, depending on the motion representation. The first group typically operates in the original skeleton feature space (composed of joints’ position, 6D representation, velocity, *etc.*). MotionDiffuse [69] is the first effort to leverage diffusion models in text-to-motion generation, while MDM [58] is a similar work that uses a Transformer [59] with fewer training parameters as the denoising network. Subsequent studies [6, 17, 22, 29, 31, 51, 60, 62, 63, 65–67, 76] employ carefully designed techniques to improve the performance of the diffusion models, such as retrieval-augmented strategy [70], discrete diffusion [33, 39], spatial-temporal attention [36, 71]. Another line of methods applies the diffusion and reverse processes in the continuous latent space. MLD [64] combines the latent diffusion model with motion VAE. GUESS [14] proposes a Gradually Enriching Synthesis strategy based on MLD. MotionMamba [73] presents a latent diffusion model with Mamba [18] architecture.

The most relevant work to ours is MLD [64], but un-

like MLD, we aim at addressing compositional motion generation by rethinking this task from an energy view. We show how our approach enables the latent diffusion model to compose complex motions from simple ones.

Compositional Generation. Compositional generation has emerged as a powerful paradigm for creating content (*e.g.*, images and motions) that combines multiple components. Our work is related to certain works in compositional image generation. Some approaches aim to develop cross-attention merging algorithms [12, 43], training strategies [5, 26, 35], and classifier guidance [15, 54], to facilitate this task. Another group of works proposes to use EBMs to compose pre-trained generative models [7, 8, 10, 37, 38, 43]. For example, Du *et al.* [8] proposed to combine independent trained energy models with several logical operators. Nie *et al.* [42] and Du *et al.* [11] introduced Ordinary Different Equation (ODE) and Markov Chain Monte Carlo (MCMC) to optimize the sampling process, respectively. In the field of motion generation, TEACH [2] and SINC [3] are pioneering works for spatial/temporal action composition based on VAE. Subsequent solutions [30, 53, 62] manipulate diffusion models to achieve more natural motion and controllability. However, they modify the reverse process in the skeleton space, which is infeasible for adapting to latent space.

Drawing inspiration from results in the image domain, we present an energy-based approach for compositional motion generation. In contrast to existing methods, we focus on exploring the motion diffusion model in continuous latent space. Through Synergistic Energy Fusion (SEF), we demonstrate the feasibility of generating high-quality, text-consistent motion by implicitly manipulating latent distributions from multiple components.

Methods	R-Precision \uparrow			FID \downarrow	MM-Dist \downarrow	Diversity \rightarrow	MModality \uparrow
	Top-1	Top-2	Top-3				
Real motion	0.424 \pm .005	0.649 \pm .006	0.779 \pm .006	0.031 \pm .004	2.788 \pm .012	11.08 \pm .097	-
MDM [58]	0.404 \pm .005	0.606 \pm .004	0.731 \pm .004	0.513 \pm .046	3.096 \pm .024	10.732 \pm .103	1.806 \pm .176
MotionDiffuse [69]	0.417 \pm .004	0.621 \pm .004	0.739 \pm .004	1.954 \pm .062	2.958 \pm .005	11.10 \pm .143	0.730 \pm .013
M2DM [33]	0.416 \pm .004	0.628 \pm .004	0.743 \pm .004	0.515 \pm .029	3.015 \pm .017	11.42 \pm .970	3.325 \pm .370
Fg-T2M [60]	0.418 \pm .005	0.626 \pm .004	0.745 \pm .004	0.571 \pm .047	3.114 \pm .015	10.93 \pm .083	1.019 \pm .029
ReMoDiffusion [70]	0.427 \pm .014	0.641 \pm .004	0.765 \pm .055	0.155 \pm .006	2.814 \pm .012	10.80 \pm .105	1.239 \pm .028
FineMoGen [71]	0.432 \pm .006	0.649 \pm .005	0.772 \pm .006	0.178 \pm .007	2.896 \pm .014	10.85 \pm .115	1.877 \pm .093
MLD* [64]	0.390 \pm .008	0.609 \pm .008	0.734 \pm .007	0.404 \pm .027	3.204 \pm .027	10.80 \pm .117	2.192 \pm .071
GUESS* [13]	0.425 \pm .003	0.632 \pm .007	0.751 \pm .005	0.371 \pm .020	2.421 \pm .022	10.93 \pm .110	2.732 \pm .084
MotionMamba* [73]	0.419 \pm .006	0.645 \pm .005	0.765 \pm .006	0.307 \pm .041	3.021 \pm .025	11.02 \pm .098	1.678 \pm .064
ENERGYMOGEN*	0.436 \pm .006	0.651 \pm .006	0.772 \pm .006	0.495 \pm .020	2.861 \pm .020	11.06 \pm .101	1.256 \pm .024

Table 2. Comparison with the state-of-the-art diffusion models on the KIT-ML [49] test set.

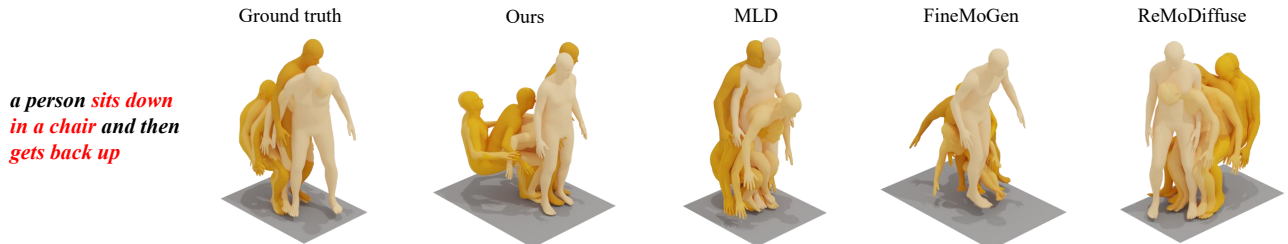


Figure 3. Visual results on the HumanML3D test set. We compare our approach with MLD [64], FineMoGen [71], and ReMoDiffuse [70]. Our approach matches the text description better. The motions generated by MLD and FineMoGen are inconsistent with “sits down in a chair”, while ReMoDiffuse fails to generate “gets back up”. More visualization results can be found on the [project page](#).

5. Experiments

We evaluate our approach on three tasks following prior studies [19, 47]: text-to-motion generation (§ 5.3), compositional motion generation (§ 5.4), and multi-concept motion generation (§ 5.4). Furthermore, we offer an in-depth dissection in § 5.5. Please kindly note that our approach can be easily generalized to skeleton-based methods. More information on datasets, evaluation metrics, training details, and the results of skeleton-based diffusion models, can be found in the appendix.

5.1. Datasets and Evaluation Metrics

Datasets. Our experiments are conducted on three datasets: HumanML3D [19], KIT-ML [49] and MTT [47]. HumanML3D and KIT-ML are used to measure the performance of text-to-motion generation. The composed texts in MTT are used for multi-concept motion generation. We utilize the original three texts and their combination generated by MTT for motion composition.

In addition to these datasets, we build **CompML**, which consists of 5000 unique motion-text pairs. We randomly select three sentences from a text set (provided in STMC [47]) to describe each motion. Then, ENERGYMOGEN composes motions based on these descriptions. We finetune

the pre-trained denoising autoencoder using both CompML and HumanML3D and evaluate it on the HumanML3D test set. We construct this dataset to show that the compositional motion generation can serve as a text-motion data augmentation approach. We also aim to demonstrate that training on motions composed by ENERGYMOGEN can benefit the text-to-motion generation (see § 5.5).

Evaluation Metrics. We use evaluation models from Guo *et al.* [19] to measure the performance of text-driven human motion generation. We adopt the same metrics as previous works, including R-Precision, MM-Dist, FID, Diversity, and MModality. For compositional motion generation and multi-concept motion generation, we follow STMC [47] to use R-Precision, TMR-Score, FID, and transition distance for evaluation.

5.2. Implementation Details

During training, the motion encoder, motion decoder, and denoising autoencoder each comprise 9 layers of transformer blocks with a dimension $d = 256$. We use 10 additional tokens (mean and various tokens) to sample $N = 5$ latent vectors representing the motion. A frozen CLIP ViT-L/14 model is applied to encode the textual descriptions. During inference, we generate motion latent vectors over 50 diffusion steps and then reconstruct them back to motion

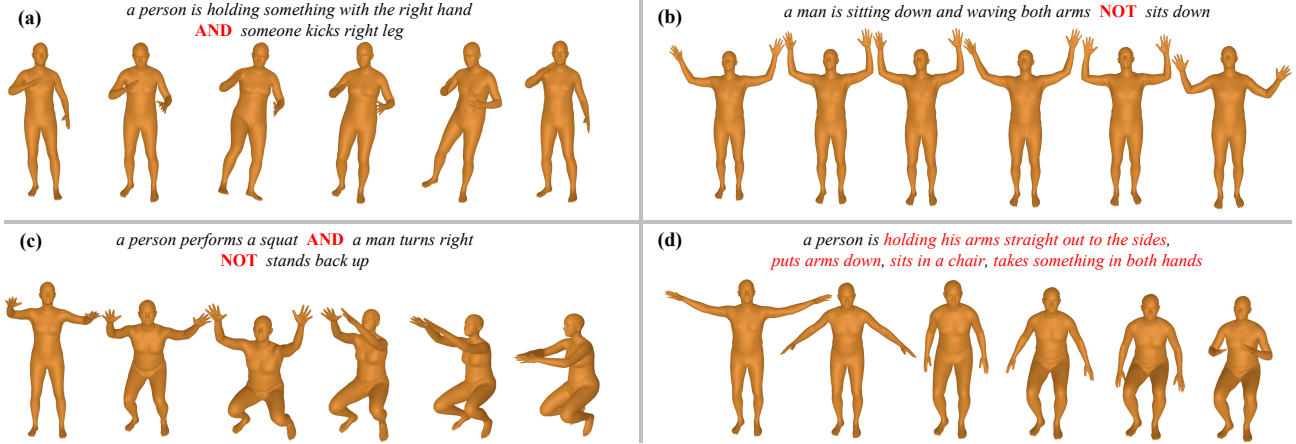


Figure 4. **Compositional motion generation.** We use the pre-trained model on HumanML3D [19] for compositional motion generation. Our approach can accurately capture the details in concepts and compose complex motions. (a) conjunction, (b) negation, (c) conjunction + negation, (d) multi-concept generation. More visual results and comparisons can be found on the [project page](#).

Methods	R-Precision		TMR-Score \uparrow		FID \downarrow	Transition distance \downarrow
	R@1 \uparrow	R@3 \uparrow	M2T	M2M		
Multi-concept motion generation (single text)						
MotionDiffuse [69]	10.9	21.3	0.558	0.546	0.621	1.9
MDM [58]	9.5	19.7	0.556	0.549	0.666	2.5
ReModiffuse [70]	7.4	18.3	0.531	0.534	0.699	3.3
FineMoGen [71]	5.4	11.7	0.504	0.533	0.948	9.4
MLD [64]	10.5	22.3	0.559	0.552	0.685	2.4
Ours	12.7	25.4	0.570	0.562	0.592	2.7
Ours + AGD	14.0	26.3	0.570	0.560	0.587	2.7
Compositional motion generation (multiple texts)						
Ours (latent only)	9.7	19.6	0.547	0.521	0.917	1.6
Ours (semantic only)	15.1	27.5	0.585	0.567	0.569	2.2
Ours + SEF	15.9	28.0	0.591	0.567	0.604	1.6

Table 3. **Quantitative comparison on MTT [47].** We compute metrics following STMC [47]. ‘AGD’ and ‘SEF’ denote the adaptive gradient descent and synergistic energy fusion.

through the motion decoder. For text-to-motion generation, γ is set to 0 for evaluation. Following [43], we split γ into $[\gamma_{attn}, \gamma_{reg}]$ for compositional and multi-concept motion generation. $[\gamma_{attn}, \gamma_{reg}]$ are set to [0.0004, 0.0004] [0.001, 0.002] for two tasks, respectively. We evaluate these two tasks on the MTT [47] dataset with the model pre-trained on HumanML3D [19]. In addition, λ_s , λ_l , and λ_m are set to 0.7, 0.1, and 0.2 for compositional generation evaluation. Ablation studies on hyper-parameters and more training details are provided in the appendix.

5.3. Experiments on Text-to-Motion Generation

Quantitative Results. Table 1 and Table 2 present the results of ENERGYMOGEN against famous skeleton-based diffusion [60, 70, 71] and latent diffusion [14, 64, 73] methods on the HumanML3D and KIT-ML test sets. Our method significantly improves the text-condition consistency and

diversity compared with the existing diffusion models while achieving competitive results on fidelity. We demonstrate that leveraging cross-attention with multiple latent vectors is crucial to this enhancement. It’s worth noting that our approach, though not initially developed for this specific task, has still demonstrated satisfactory performance.

Qualitative Results. Figure 3 shows visual results on HumanML3D [19]. We compare ENERGYMOGEN with MLD [64] and current state-of-the-art skeleton-based methods: ReMoDiffuse [70] and FineMoGen [71]. It can be seen that the motion generated by our approach is more consistent with the textual description. FineMoGen generates some unrealistic frames, and both FineMoGen and MLD fail to generate “sits down in a chair”. The generated motion of ReMoDiffuse [70] is not related to “gets back up”.

5.4. Experiments on Motion Composition

Quantitative Results. In Table 3, we perform a comprehensive comparison against two divergent groups of diffusion models (*i.e.*, skeleton-based and latent-based) on the MTT dataset. We empirically find that the motion jitter issue in FineMoGen [71] and ReMoDiffuse [70] hinders their performance on this task. Our approach outperforms both types of rivals on multi-concept and compositional motion generation tasks. Precisely, ENERGYMOGEN with adaptive gradient descent of text embeddings (in Equation 4) outperforms previous state-of-the-art methods on R-Precision, TMR-Score, and FID. With synergistic energy fusion, ENERGYMOGEN significantly exhibits significant performance advantages over all prior methods.

Qualitative Results. In Figure 4, we show visual results of compositional motion generation in four settings: (a) conjunction, (b) negation, (c) conjunction + negation, and (d) multi-concept generation. Our approach can generate high-quality motions that are consistent with multiple concepts.

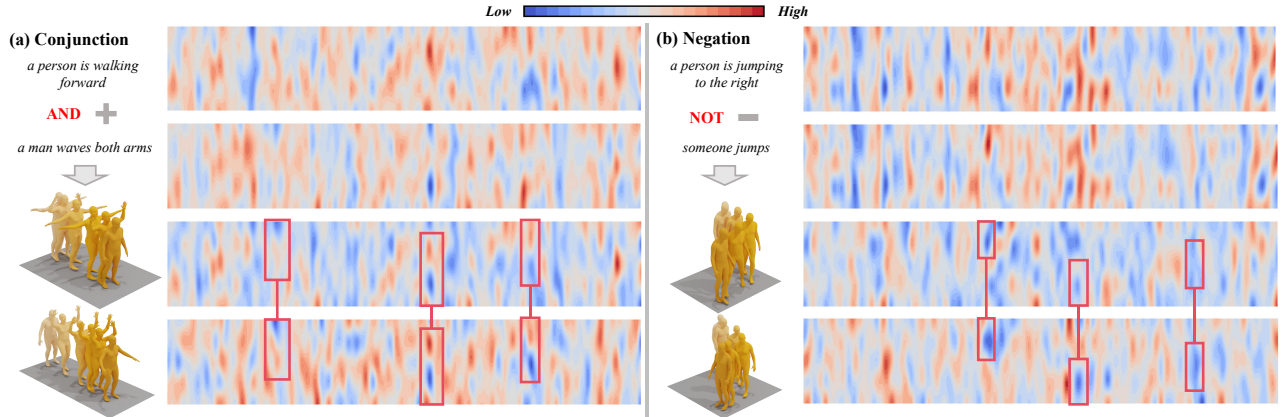


Figure 5. **Analysis of the latent distribution.** For a clear illustration, energy distributions are calculated with interpolation and Gaussian smoothing, then visualized as contour maps. Motions in the 4th row are generated from texts, *i.e.*, “a person is walking forward and waving both arms” and “a person is walking to the right”, which is created by composing the multiple concepts into a single text via (a) Conjunction and (b) Negation. Similar regions are highlighted in red.

5.5. In-Depth Dissection of ENERGYMOGEN

Key Component Analysis. We first investigate the key components in our ENERGYMOGEN.

Q1: Does the adaptive gradient descent alleviate the issue of text inconsistency in multi-concept motion generation? *Yes.* As shown in Table 3, our approach with adaptive updating of the textual embedding aligns better with textual descriptions. It improves the R-Precision by 1.3% and 0.9% for Top1 and Top3 accuracy, respectively. Meanwhile, we achieve better FID and comparable results on the TMR-Score and transition distance. The ablation study of $[\gamma_{attn}, \gamma_{reg}]$ and qualitative comparisons are provided in Section E of the appendix.

Q2: What roles do latent-aware and semantic-aware EBMs play in motion composition? To answer this question, we conduct ablative experiments on MTT [47], results are shown in Table 3. One can figure out that the semantic-aware EBM significantly enhances the text-motion consistency, but it suffers from foot slides and motion jitter. Although the latent-aware method performs poorly on R-Precision and TMR Score, it clearly decreases the transition distance. We notice that Synergistic Energy Fusion (SEF) effectively alleviates these issues by leveraging the complementary strengths of the two spectrums. We present visual results and ablation studies on λ_s , λ_l , and λ_m in Section C of the appendix.

Q3: How does ENERGYMOGEN compose complex motions through energy? We study the underlying mechanism of our approach from the perspectives of **conjunction** and **negation**. We visualize the energy distributions of motion latent representations generated from the denoising autoencoder in Figure 5. In concept conjunction, we add the two distributions together, and the contour maps from compositional generation (the 3rd row) and multi-concept

generation (the last row) demonstrate consistent high- and low-energy regions. In concept negation, we input a text of “a person is walking to the right” based on the motion generated by composing “a person is jumping to the right” and “someone jumps”. Despite the absence of “walking” in the original concepts, the energy distributions of the two motions (the 3rd and 4th rows) still exhibit similar regions. Similar energy regions are highlighted in red. Such results potentially explain the effectiveness of ENERGYMOGEN.

Experiments on CompML. We finetune the pretrained denoising network using both HumanML3D and CompML. The results are illustrated in Table 1. We observe that the model’s performance improves with additional training data from CompML. Our experiments demonstrate that compositional motion generation can be effectively employed as a data augmentation technique. Furthermore, such results also indicate that the motions generated by our approach are of sufficient quality to be used for data augmentation.

6. Conclusion

In this paper, we present a framework for compositional human motion generation, aiming at composing complex motions from a set of simple concepts. We explore an energy-based regime where the denoising autoencoder and cross-attention are interpreted as energy functions for latent-aware and semantic-aware composition, and energy distributions are combined in latent space through Synergistic Energy Fusion. Our approach consistently shows superior performance across various tasks on several commonly used benchmarks. Extensive investigations demonstrate that our approach is general, effective and interpretable. Moreover, we build a dataset and suggest motion composition as a data augmentation technique, which can bring additional improvement to text-to-motion generation.

References

- [1] Chaitanya Ahuja and Louis-Philippe Morency. Language2pose: Natural language grounded pose forecasting. In *International Conference on 3D Vision (3DV)*, 2019. 5
- [2] Nikos Athanasiou, Mathis Petrovich, Michael J. Black, and Gül Varol. TEACH: Temporal Action Compositions for 3D Humans. In *International Conference on 3D Vision (3DV)*, 2022. 1, 5, 15
- [3] Nikos Athanasiou, Mathis Petrovich, Michael J. Black, and Gül Varol. SINC: Spatial composition of 3D human motions for simultaneous action generation. In *Proceedings of the International Conference on Computer Vision (ICCV)*, 2023. 1, 5
- [4] Michael Ayers. Locke: Epistemology and ontology. *Routledge*, 1991. 1
- [5] Yuren Cong, Martin Renqiang Min, Li Erran Li, Bodo Rosenhahn, and Michael Ying Yang. Attribute-centric compositional text-to-image generation. *arXiv preprint arXiv:2301.01413*, 2023. 5
- [6] Rishabh Dabral, Muhammad Hamza Mughal, Vladislav Golyanik, and Christian Theobalt. Mofusion: A framework for denoising-diffusion-based motion synthesis. In *Proceedings of the Conference on Computer Vision and Pattern Recognition (CVPR)*, 2023. 5
- [7] Yilun Du and Igor Mordatch. Implicit generation and modeling with energy based models. *Advances in Neural Information Processing Systems (NeurIPS)*, 2019. 1, 2, 3, 5
- [8] Yilun Du, Shuang Li, and Igor Mordatch. Compositional visual generation with energy based models. *Advances in Neural Information Processing Systems (NeurIPS)*, 2020. 3, 4, 5
- [9] Yilun Du, Shuang Li, Joshua Tenenbaum, and Igor Mordatch. Improved contrastive divergence training of energy based models. *arXiv preprint arXiv:2012.01316*, 2020. 1, 2
- [10] Yilun Du, Shuang Li, Yash Sharma, Josh Tenenbaum, and Igor Mordatch. Unsupervised learning of compositional energy concepts. *Advances in Neural Information Processing Systems (NeurIPS)*, 2021. 5
- [11] Yilun Du, Conor Durkan, Robin Strudel, Joshua B Tenenbaum, Sander Dieleman, Rob Fergus, Jascha Sohl-Dickstein, Arnaud Doucet, and Will Sussman Grathwohl. Reduce, reuse, recycle: Compositional generation with energy-based diffusion models and mcmc. In *International Conference on Machine Learning (ICML)*, 2023. 1, 2, 5
- [12] Weixi Feng, Xuehai He, Tsu-Jui Fu, Varun Jampani, Arjun Reddy Akula, Pradyumna Narayana, Sugato Basu, Xin Eric Wang, and William Yang Wang. Training-free structured diffusion guidance for compositional text-to-image synthesis. In *International Conference on Learning Representations (ICLR)*, 2023. 5
- [13] Xuehao Gao, Yang Yang, Zhenyu Xie, Shaoyi Du, Zhongqian Sun, and Yang Wu. Guess gradually enriching synthesis for text-driven human motion generation. *IEEE Transactions on Visualization and Computer Graphics*, 2024. 5, 6
- [14] Xuehao Gao, Yang Yang, Zhenyu Xie, Shaoyi Du, Zhongqian Sun, and Yang Wu. Guess: Gradually enriching synthesis for text-driven human motion generation. *IEEE Transactions on Visualization and Computer Graphics*, 2024. 5, 7
- [15] Timur Garipov, Sebastiaan De Peuter, Ge Yang, Vikas Garg, Samuel Kaski, and Tommi Jaakkola. Compositional sculpting of iterative generative processes. *Advances in Neural Information Processing Systems (NeurIPS)*, 2023. 5
- [16] Anindita Ghosh, Noshaba Cheema, Cennet Oguz, Christian Theobalt, and Philipp Slusallek. Synthesis of compositional animations from textual descriptions. In *Proceedings of the International Conference on Computer Vision (ICCV)*, 2021. 5
- [17] Purvi Goel, Kuan-Chieh Wang, C Karen Liu, and Kayvon Fatahalian. Iterative motion editing with natural language. In *ACM SIGGRAPH 2024 Conference Papers*, 2024. 5
- [18] Albert Gu and Tri Dao. Mamba: Linear-time sequence modeling with selective state spaces. *arXiv preprint arXiv:2312.00752*, 2023. 5
- [19] Chuan Guo, Shihao Zou, Xinxin Zuo, Sen Wang, Wei Ji, Xingyu Li, and Li Cheng. Generating diverse and natural 3d human motions from text. In *Proceedings of the Conference on Computer Vision and Pattern Recognition (CVPR)*, 2022. 2, 5, 6, 7, 12, 13, 14, 15
- [20] Chuan Guo, Xinxin Zuo, Sen Wang, and Li Cheng. Tm2t: Stochastic and tokenized modeling for the reciprocal generation of 3d human motions and texts. In *Proceedings of the European Conference on Computer Vision (ECCV)*, 2022. 5
- [21] Chuan Guo, Yuxuan Mu, Muhammad Gohar Javed, Sen Wang, and Li Cheng. Momask: Generative masked modeling of 3d human motions. In *Proceedings of the Conference on Computer Vision and Pattern Recognition (CVPR)*, 2024. 5
- [22] Bo Han, Hao Peng, Minjing Dong, Yi Ren, Yixuan Shen, and Chang Xu. Amd: Autoregressive motion diffusion. In *Proceedings of the AAAI Conference on Artificial Intelligence*, 2024. 5
- [23] Jonathan Ho and Tim Salimans. Classifier-free diffusion guidance. *arXiv preprint arXiv:2207.12598*, 2022. 2, 4, 12
- [24] Jonathan Ho, Ajay Jain, and Pieter Abbeel. Denoising diffusion probabilistic models. In *Advances in Neural Information Processing Systems (NeurIPS)*, 2020. 1
- [25] Benjamin Hoover, Yuchen Liang, Bao Pham, Rameswar Panda, Hendrik Strobelt, Duen Horng Chau, Mohammed Zaki, and Dmitry Krotov. Energy transformer. *Advances in Neural Information Processing Systems (NeurIPS)*, 2024. 2, 3
- [26] Lianghua Huang, Di Chen, Yu Liu, Yujun Shen, Deli Zhao, and Jingren Zhou. Composer: Creative and controllable image synthesis with composable conditions. *arXiv preprint arXiv:2302.09778*, 2023. 5
- [27] Aapo Hyvärinen and Peter Dayan. Estimation of non-normalized statistical models by score matching. *Journal of Machine Learning Research (JMLR)*, 2005. 2
- [28] Biao Jiang, Xin Chen, Wen Liu, Jingyi Yu, Gang Yu, and Tao Chen. Motiongpt: Human motion as a foreign language. *arXiv*, 2023. 5

- [29] Peng Jin, Yang Wu, Yanbo Fan, Zhongqian Sun, Wei Yang, and Li Yuan. Act as you wish: Fine-grained control of motion diffusion model with hierarchical semantic graphs. *Advances in Neural Information Processing Systems (NeurIPS)*, 2023. 5
- [30] Korrawe Karunratanakul, Konpat Preechakul, Supasorn Suwajanakorn, and Siyu Tang. Guided motion diffusion for controllable human motion synthesis. In *Proceedings of the International Conference on Computer Vision (ICCV)*, 2023. 5
- [31] Korrawe Karunratanakul, Konpat Preechakul, Supasorn Suwajanakorn, and Siyu Tang. Guided motion diffusion for controllable human motion synthesis. In *Proceedings of the International Conference on Computer Vision (ICCV)*, 2023. 1, 5
- [32] Diederik P Kingma and Max Welling. Auto-encoding variational bayes. In *International Conference on Learning Representations (ICLR)*, 2014. 3
- [33] Hanyang Kong, Kehong Gong, Dongze Lian, Michael Bi Mi, and Xinchao Wang. Priority-centric human motion generation in discrete latent space. In *Proceedings of the Conference on Computer Vision and Pattern Recognition (CVPR)*, 2023. 5, 6
- [34] Yann LeCun, Sumit Chopra, Raia Hadsell, M Ranzato, Fujie Huang, et al. A tutorial on energy-based learning. *Predicting structured data*, 2006. 1, 2
- [35] Zhiheng Li, Martin Renqiang Min, Kai Li, and Chenliang Xu. Stylet2i: Toward compositional and high-fidelity text-to-image synthesis. In *Proceedings of the Conference on Computer Vision and Pattern Recognition (CVPR)*, 2022. 5
- [36] Chang Liu, Mengyi Zhao, Bin Ren, Mengyuan Liu, Nicu Sebe, et al. Spatio-temporal graph diffusion for text-driven human motion generation. In *Proceedings of the British Machine Vision Conference (BMVC)*, 2023. 5
- [37] Nan Liu, Shuang Li, Yilun Du, Josh Tenenbaum, and Antonio Torralba. Learning to compose visual relations. *Advances in Neural Information Processing Systems (NeurIPS)*, 2021. 5
- [38] Nan Liu, Shuang Li, Yilun Du, Antonio Torralba, and Joshua B Tenenbaum. Compositional visual generation with composable diffusion models. In *Proceedings of the European Conference on Computer Vision (ECCV)*, 2022. 3, 4, 5
- [39] Yunhong Lou, Linchao Zhu, Yaxiong Wang, Xiaohan Wang, and Yi Yang. Diversemotion: Towards diverse human motion generation via discrete diffusion. *arXiv preprint arXiv:2309.01372*, 2023. 5
- [40] Shunlin Lu, Ling-Hao Chen, Ailing Zeng, Jing Lin, Ruimao Zhang, Lei Zhang, and Heung-Yeung Shum. Humantomato: Text-aligned whole-body motion generation. *arxiv:2310.12978*, 2023. 5
- [41] Naureen Mahmood, Nima Ghorbani, Nikolaus F Troje, Gerard Pons-Moll, and Michael J Black. Amass: Archive of motion capture as surface shapes. In *Proceedings of the International Conference on Computer Vision (ICCV)*, 2019. 14
- [42] Weili Nie, Arash Vahdat, and Anima Anandkumar. Controllable and compositional generation with latent-space energy-based models. *Advances in Neural Information Processing Systems (NeurIPS)*, 2021. 5
- [43] Geon Yeong Park, Jeongsol Kim, Beomsu Kim, Sang Wan Lee, and Jong Chul Ye. Energy-based cross attention for bayesian context update in text-to-image diffusion models. *Advances in Neural Information Processing Systems (NeurIPS)*, 2024. 1, 2, 3, 5, 7, 13
- [44] Mathis Petrovich, Michael J. Black, and Gül Varol. Action-conditioned 3D human motion synthesis with transformer VAE. In *Proceedings of the International Conference on Computer Vision (ICCV)*, 2021. 5
- [45] Mathis Petrovich, Michael J. Black, and Gul Varol. TEMOS: Generating diverse human motions from textual descriptions. In *Proceedings of the European Conference on Computer Vision (ECCV)*, 2022.
- [46] Mathis Petrovich, Michael J Black, and Gül Varol. Tmr: Text-to-motion retrieval using contrastive 3d human motion synthesis. In *Proceedings of the International Conference on Computer Vision (ICCV)*, 2023. 5, 15
- [47] Mathis Petrovich, Or Litany, Umar Iqbal, Michael J. Black, Gül Varol, Xue Bin Peng, and Davis Rempe. Multi-track timeline control for text-driven 3d human motion generation. In *Proceedings of the Conference on Computer Vision and Pattern Recognition Workshops (CVPRW)*, 2024. 2, 6, 7, 8, 12, 14, 15
- [48] Ekkasit Pinyoanuntapong, Pu Wang, Minwoo Lee, and Chen Chen. Mmm: Generative masked motion model. In *Proceedings of the Conference on Computer Vision and Pattern Recognition (CVPR)*, 2024. 5
- [49] Matthias Plappert, Christian Mandery, and Tamim Asfour. The kit motion-language dataset. *Big data*, 2016. 2, 6, 14
- [50] Hubert Ramsauer, Bernhard Schödl, Johannes Lehner, Philipp Seidl, Michael Widrich, Thomas Adler, Lukas Gruber, Markus Holzleitner, Milena Pavlović, Geir Kjetil Sandve, et al. Hopfield networks is all you need. *arXiv preprint arXiv:2008.02217*, 2020. 2, 3
- [51] Zeping Ren, Shaoli Huang, and Xiu Li. Realistic human motion generation with cross-diffusion models. *arXiv preprint arXiv:2312.10993*, 2023. 5
- [52] Robin Rombach, Andreas Blattmann, Dominik Lorenz, Patrick Esser, and Björn Ommer. High-resolution image synthesis with latent diffusion models. In *Proceedings of the Conference on Computer Vision and Pattern Recognition (CVPR)*, 2022. 1
- [53] Yoni Shafir, Guy Tevet, Roy Kapon, and Amit Haim Bermano. Human motion diffusion as a generative prior. In *International Conference on Learning Representations (ICLR)*, 2024. 1, 5, 12, 13
- [54] Changhao Shi, Haomiao Ni, Kai Li, Shaobo Han, Mingfu Liang, and Martin Renqiang Min. Exploring compositional visual generation with latent classifier guidance. In *Proceedings of the Conference on Computer Vision and Pattern Recognition (CVPR)*, 2023. 5
- [55] Jascha Sohl-Dickstein, Eric Weiss, Niru Maheswaranathan, and Surya Ganguli. Deep unsupervised learning using

- nonequilibrium thermodynamics. In *International Conference on Machine Learning (ICML)*, 2015. 1
- [56] Yang Song, Jascha Sohl-Dickstein, Diederik P Kingma, Abhishek Kumar, Stefano Ermon, and Ben Poole. Score-based generative modeling through stochastic differential equations. *arXiv preprint arXiv:2011.13456*, 2020. 2
- [57] Guy Tevet, Brian Gordon, Amir Hertz, Amit H Bermano, and Daniel Cohen-Or. Motionclip: Exposing human motion generation to clip space. In *Proceedings of the European Conference on Computer Vision (ECCV)*, 2022. 5
- [58] Guy Tevet, Sigal Raab, Brian Gordon, Yonatan Shafir, Amit H Bermano, and Daniel Cohen-Or. Human motion diffusion model. *arXiv*, 2022. 1, 5, 6, 7, 13, 14
- [59] Ashish Vaswani, Noam Shazeer, Niki Parmar, Jakob Uszkoreit, Llion Jones, Aidan N Gomez, Łukasz Kaiser, and Illia Polosukhin. Attention is all you need. In *Advances in Neural Information Processing Systems (NeurIPS)*, 2017. 5
- [60] Yin Wang, Zhiying Leng, Frederick WB Li, Shun-Cheng Wu, and Xiaohui Liang. Fg-t2m: Fine-grained text-driven human motion generation via diffusion model. In *Proceedings of the International Conference on Computer Vision (ICCV)*, 2023. 1, 5, 6, 7
- [61] Max Welling and Yee W Teh. Bayesian learning via stochastic gradient langevin dynamics. In *International Conference on Machine Learning (ICML)*, 2011. 3
- [62] Yiming Xie, Varun Jampani, Lei Zhong, Deqing Sun, and Huaizu Jiang. Omnicontrol: Control any joint at any time for human motion generation. *arXiv preprint arXiv:2310.08580*, 2023. 5
- [63] Zhenyu Xie, Yang Wu, Xuehao Gao, Zhongqian Sun, Wei Yang, and Xiaodan Liang. Towards detailed text-to-motion synthesis via basic-to-advanced hierarchical diffusion model. In *Proceedings of the AAAI Conference on Artificial Intelligence*, 2024. 5
- [64] Chen Xin, Biao Jiang, Wen Liu, Zilong Huang, Bin Fu, Tao Chen, Jingyi Yu, and Gang Yu. Executing your commands via motion diffusion in latent space. *arXiv*, 2022. 1, 3, 5, 6, 7
- [65] Zhao Yang, Bing Su, and Ji-Rong Wen. Synthesizing long-term human motions with diffusion models via coherent sampling. In *Proceedings of the ACM International Conference on Multimedia (ACMMM)*, 2023. 5
- [66] Ye Yuan, Jiaming Song, Umar Iqbal, Arash Vahdat, and Jan Kautz. Physdiff: Physics-guided human motion diffusion model. In *Proceedings of the International Conference on Computer Vision (ICCV)*, 2023.
- [67] Yuanhao Zhai, Mingzhen Huang, Tianyu Luan, Lu Dong, Ifeoma Nwogu, Siwei Lyu, David Doermann, and Jun-song Yuan. Language-guided human motion synthesis with atomic actions. In *Proceedings of the ACM International Conference on Multimedia (ACMMM)*, 2023. 5
- [68] Jianrong Zhang, Yangsong Zhang, Xiaodong Cun, Yong Zhang, Hongwei Zhao, Hongtao Lu, Xi Shen, and Ying Shan. Generating human motion from textual descriptions with discrete representations. In *Proceedings of the Conference on Computer Vision and Pattern Recognition (CVPR)*, 2023. 3, 5
- [69] Mingyuan Zhang, Zhongang Cai, Liang Pan, Fangzhou Hong, Xinying Guo, Lei Yang, and Ziwei Liu. Motiondiffuse: Text-driven human motion generation with diffusion model. *arXiv*, 2022. 5, 6, 7, 12, 13, 14
- [70] Mingyuan Zhang, Xinying Guo, Liang Pan, Zhongang Cai, Fangzhou Hong, Huirong Li, Lei Yang, and Ziwei Liu. Remodiffuse: Retrieval-augmented motion diffusion model. *arXiv*, 2023. 1, 5, 6, 7, 12, 13, 14
- [71] Mingyuan Zhang, Huirong Li, Zhongang Cai, Jiawei Ren, Lei Yang, and Ziwei Liu. Finemogen: Fine-grained spatio-temporal motion generation and editing. *Advances in Neural Information Processing Systems (NeurIPS)*, 2023. 1, 5, 6, 7, 12, 13, 14
- [72] Yaqi Zhang, Di Huang, Bin Liu, Shixiang Tang, Yan Lu, Lu Chen, Lei Bai, Qi Chu, Nenghai Yu, and Wanli Ouyang. Motiongpt: Finetuned llms are general-purpose motion generators. *arXiv*, 2023. 5
- [73] Zeyu Zhang, Akide Liu, Ian Reid, Richard Hartley, Bohan Zhuang, and Hao Tang. Motion mamba: Efficient and long sequence motion generation. In *European Conference on Computer Vision*, pages 265–282. Springer, 2025. 5, 6, 7, 13
- [74] Junbo Zhao, Michael Mathieu, and Yann LeCun. Energy-based generative adversarial networks. In *International Conference on Learning Representations (ICLR)*, 2017. 1, 2
- [75] Chongyang Zhong, Lei Hu, Zihao Zhang, and Shihong Xia. Att2m: Text-driven human motion generation with multi-perspective attention mechanism. In *Proceedings of the International Conference on Computer Vision (ICCV)*, 2023. 5
- [76] Zixiang Zhou and Baoyuan Wang. Ude: A unified driving engine for human motion generation. In *Proceedings of the Conference on Computer Vision and Pattern Recognition (CVPR)*, 2023. 5

Appendix

In this appendix, we present:

- Section **A**: Training details of ENERGYMOGEN.
- Section **B**: Additional results of skeleton-based diffusion models.
- Section **C**: Ablations on λ_s , λ_l , and λ_m for Synergistic Energy Fusion.
- Section **D**: Ablations on the number of latent vectors in motion VAE.
- Section **E**: Ablation study of hyper-parameters in energy-based cross-attention.
- Section **F**: More visual results of energy distributions.
- Section **G**: More details on datasets and evaluation metrics.

A. Implementation Details

We first provide training details of ENERGYMOGEN. For Motion VAE, both the encoder \mathcal{E} and decoder \mathcal{D} comprise 9 layers of transformer blocks with a dimension $d=256$. We use 10 additional tokens (mean and various tokens) to sample $N=5$ latent vectors representing the motion. We use an AdamW optimizer with a batch size of 1024. We train 300K iterations in total, and the learning rate changes from 0.0001 to 0.00001 after 200K iterations. The weights of reconstruction loss and KL loss are set to 1 and 0.0001. As for the latent diffusion, we apply a frozen CLIP ViT-L/14 to encode the textual descriptions. Regarding the denoising autoencoder, we use a 9-layer transformer with a dimension of 256. To acquire an accurate mapping from textual data to latent vectors during training, γ is initialized with 0. We utilize the AdamW optimizer to train the model with a batch size of 512, with an initial learning rate of 0.0001 for 200K iterations and decayed to 0.00001 for another 100K iterations. The diffusion model is learned using classifier-free guidance [23] with an unconditional score estimation rate of 10%. For experiments on CompML, we only finetune the latent diffusion model for 100K iterations in total with a learning rate of 0.00005.

For the skeleton-based approach, we use an 8-layer transformer with a dimension of 512. We follow [69] to train the model using Adam optimizer with a batch size of 1024. We train 8000 epochs in total and employ

the CosineAnnealing learning policy with the learning rate from 0.0002 to 0.00002.

B. Additional Results of Skeleton-Based Diffusion Models

B.1. Text-to-Motion Generation

We conduct experiments on HumanML3D [19] to evaluate the performance of text-to-motion generation. We use evaluation models from Guo *et al.* [19] and use the same metrics. The training details of skeleton-based ENERGYMOGEN are provided in Section A. Experimental results are shown in Table 4. Our approach outperforms current state-of-the-art skeleton-based methods, *i.e.*, ReMoDiffuse [70] and FineMoGen [71] on R-Precision, Diversity, and MM-Dist, while achieves comparable results on FID and MModality.

B.2. Motion Temporal Composition

Following FineMoGen [71] and PriorMDM [53], we use the motion temporal composition task to measure the compositional capacity of our approach. We perform latent-aware composition to tackle this task.

Specifically, denoting c_1 and c_2 as two concepts. $M_{c_1}^t \in \mathbb{R}^{N_1 \times d_m}$, $M_{c_2}^t \in \mathbb{R}^{N_2 \times d_m}$ denote predicted scores corresponding to two concepts at t -th step, N_i is the motion length, and d_m is the dimension of motions. $M_3^t \in \mathbb{R}^{N' \times d_m}$ indicates the overlapping part, where N' is the number of interval frame. Each reverse process can be formulated as:

$$\begin{aligned} M_{c_1, c_2}^t &= M_{c_1}^t[: N_1 - N'] \oplus (M_{c_1}^t[N_1 - N'] :) + \\ &M_{c_2}^t[: N'] - M_3^t \oplus M_{c_2}^t[N'] :, \end{aligned} \quad (11)$$

where M_{c_1, c_2}^t is the final score at t -th step, \oplus is the concatenate operation. We conduct experiments on the HumanML3D dataset, and the results are shown in Table 5. We implement MotionDiffuse [69], ReMoDiffuse [70], and FineMoGen [71] using the “first take” from PriorMDM [53]. Our approach is implemented based on Equation 11, and exhibits performance advantages compared with previous methods. We provide visual comparisons with PriorMDM, which can be found on the [project page](#).

B.3. Multi-Concept Motion Generation

In Table 6, we show quantitative results on the MTT [47] dataset. Our approach without Adaptive Gradient Descent (AGD) yields results that are competitive with existing state-of-the-art methods. By combining AGD, our approach achieves superior performance on R-Precision, TMR-Score, and Transition distance.

C. Ablations on Synergistic Energy Fusion

We show the effect of hyper-parameters λ_l , λ_s , and λ_m (*c.f.*, Equation 10) in Table 7. The results in the first three rows

Methods	R-Precision \uparrow			FID \downarrow	MM-Dist \downarrow	Diversity \rightarrow	MModality \uparrow
	Top-1	Top-2	Top-3				
Real motion	0.511 \pm .003	0.703 \pm .003	0.797 \pm .002	0.002 \pm .000	2.974 \pm .008	9.503 \pm .065	-
MDM [58]	0.418 \pm .005	0.604 \pm .001	0.707 \pm .004	0.489 \pm .025	3.630 \pm .023	9.450 \pm .066	2.870 \pm 1.11
MotionDiffuse [69]	0.491 \pm .001	0.681 \pm .001	0.782 \pm .001	0.630 \pm .001	3.113 \pm .001	<u>9.410</u> \pm .049	1.553 \pm .042
ReMoDiffusion [70]	<u>0.510</u> \pm .005	<u>0.698</u> \pm .006	<u>0.795</u> \pm .004	0.103 \pm .004	<u>2.974</u> \pm .016	9.018 \pm .075	1.795 \pm .043
FineMoGen [71]	0.504 \pm .002	0.690 \pm .002	0.784 \pm .004	0.151 \pm .008	2.998 \pm .008	9.263 \pm .094	<u>2.696</u> \pm .079
ENERGYMOGEN (skeleton)	0.528 \pm .003	0.718 \pm .003	0.810 \pm .002	<u>0.139</u> \pm .007	2.902 \pm .010	9.386 \pm .078	2.549 \pm 0.104

Table 4. **Comparison with the state-of-the-art diffusion models on the HumanML3D [19] test set.** We repeat the evaluation 20 times for each metric and report the average with a 95% confidence interval. Bold and underlined indicate the best and second-best results.

Methods	R-Precision \uparrow	FID \downarrow	Diversity \rightarrow	MM-Dist \downarrow
Ground Truth	0.80	1.6×10^{-3}	9.62	2.96
PriorMDM [53] (Double take)	0.59	0.60	<u>9.50</u>	5.61
PriorMDM [53] (First take)	0.59	1.00	<u>9.46</u>	5.63
MotionDiffuse [73]	0.62	1.76	8.55	5.40
ReMoDiffuse [70]	<u>0.64</u>	0.40	9.35	<u>5.24</u>
FineMoGen [53]	<u>0.64</u>	0.45	9.23	5.27
Ours	0.67	<u>0.43</u>	9.52	5.22

Table 5. **Quantitative results on the HumanML3D [19] test set.** R-Precision denotes Top-3 accuracy. Bold and underlined indicate the best and second-best results.

correspond to ‘‘Ours (latent only)’’, ‘‘Ours (semantic only)’’, and ‘‘Ours’’ in Table 3, respectively.

Then we conduct ablative experiments on the weights of the two spectra of the energy-based model (latent-aware and semantic-aware), as shown in the middle five rows (Table 7). We find that as the weight of λ_s increases, the results align more closely with the text (R-Precision and TMR-Score), while larger weights for λ_l produce smoother motions (Transition distance). This further validates our conclusions in the main paper (Section 5.5 Q2).

Meanwhile, we also demonstrate that combining multi-concept motion generation can further improve the performance, as shown in the last 4 rows. It can be seen that Synergistic Energy Fusion with $\lambda_l = 0.1$, $\lambda_s = 0.7$, and $\lambda_m = 0.2$ achieves best performance.

D. Ablations on the Number of Latent Vectors N in Motion VAE

The results are provided in Table 8. For reconstruction, 7 latent vectors achieve the best results. However, it increases the difficulty of latent diffusion models in training. Using 5 latent vectors to represent the motion obtains the best text-to-motion generation performance.

E. Ablation Study of Hyper-parameters in Cross-Attention

We investigate the impact of γ_{attn} and γ_{reg} (*c.f.*, Equation 4, we follow [43] to split γ into attention step size γ_{attn} and regularization step size γ_{reg} for compositional and multi-concept motion generation) in energy-based cross-attention, and the results are presented in Table 9. We notice that $\gamma_{attn}, \gamma_{reg} \geq 0.1$ significantly degrades the performance, and $\gamma_{attn}, \gamma_{reg} = [0.001, 0.002]$ achieves best results on MTT (Section 5.5 Q1).

F. Energy Distribution Visualization

We show additional contour maps of energy distributions in Figure 6. We provide two examples of the concept conjunction. We visualize the energy distributions of motion latent representations generated from the denoising autoencoder. Multi-concept generation combines concepts from both (a) and (b). Compared with multi-concept generation (*i.e.*, (d) in Figure 6), energy distributions of composed motion (*i.e.*, (c) in Figure 6) show consistent high- and low-energy regions. This demonstrates that complex motion latent distributions can be composed of a set of simple distributions, which also indicates that our method is explainable. Such results further explain the effectiveness of ENERGYMOGEN (Section 5.5 Q3).

Methods	R-Precision		TMR-Score \uparrow		FID \downarrow	Transition distance \downarrow
	R@1 \uparrow	R@3 \uparrow	M2T	M2M		
MotionDiffuse [69]	<u>10.9</u>	21.3	<u>0.558</u>	0.546	0.621	1.9
MDM [58]	9.5	19.7	0.556	<u>0.549</u>	0.666	2.5
ReModiffuse [70]	7.4	18.3	0.531	0.534	0.699	3.3
FineMoGen [71]	5.4	11.7	0.504	0.533	0.948	9.4
ENERGYMOGEN (skeleton)	11.5	<u>22.6</u>	0.550	<u>0.549</u>	0.670	<u>2.2</u>
ENERGYMOGEN (skeleton) + AGD	11.5	24.4	0.560	0.552	<u>0.643</u>	1.9

Table 6. **Quantitative comparison of skeleton-based diffusion on MTT [47]**. We compute metrics following STMC [47]. ‘AGD’ denotes the adaptive gradient descent

λ_l	λ_s	λ_m	Per-crop semantic correctness				Realism	
			R@1 \uparrow	R@3 \uparrow	TMR-Score \uparrow M2T	M2M	FID \downarrow	Transition distance \downarrow
1.0	0.0	0.0	9.7	19.6	0.547	0.521	0.917	1.6
0.0	1.0	0.0	<u>15.1</u>	<u>27.5</u>	0.585	0.567	0.569	2.2
0.0	0.0	1.0	12.7	25.4	0.570	0.562	<u>0.592</u>	2.7
0.5	0.5	0.0	13.3	25.5	0.584	0.551	0.740	1.4
0.4	0.6	0.0	12.7	25.0	0.584	0.555	0.730	1.4
0.3	0.7	0.0	13.4	26.4	0.589	0.559	0.694	1.4
0.2	0.8	0.0	13.6	26.9	<u>0.590</u>	0.558	0.668	<u>1.5</u>
0.1	0.9	0.0	14.2	<u>27.5</u>	0.587	<u>0.563</u>	0.613	1.7
0.3	0.4	0.3	14.5	27.1	0.588	0.560	0.669	1.6
0.2	0.5	0.3	14.4	26.9	<u>0.590</u>	<u>0.563</u>	0.628	1.6
0.1	0.7	0.2	15.7	28.0	0.591	0.567	0.604	1.6
0.1	0.8	0.1	14.9	26.7	0.587	<u>0.563</u>	0.615	1.6

Table 7. **Ablation of hyper-parameters in Synergistic Energy Fusion on MTT [47]**. We find that as the weight of λ_s increases, the results align more closely with the text (R-Precision and TMR-Score), while larger weights for λ_l produce smoother motions (Transition distance).

G. More Details on Datasets and Evaluation Metrics

G.1. Datasets

Our experiments are conducted on three datasets: HumanML3D [19], KIT-ML [49], and MTT [47].

- **HumanML3D [19]** is a large-scale text-to-motion generation benchmark that contains 14,616 human motions with 44,970 textual descriptions. The dataset is split with proportions of 80%, 5%, and 15% for training, validation, and testing, respectively.
- **KIT-ML [49]** is another leading benchmark for motion generation from relatively short text. It has 3,911 finely annotated human motions, with 4888/300/830 for the training, validation, and test sets.
- **MTT [47]** has 60 textual descriptions with body part annotations. The corresponding motions are collected from

the AMASS dataset [41]. Three texts are randomly composed based on body parts and motion duration through some conjunction words (e.g., “and”, “while”), resulting in a test set with 500 samples.

The three datasets use the same motion representation proposed in HumanML3D [19].

G.2. Evaluation Metrics

We use evaluation models from Guo *et al.* [19] to measure the performance of text-driven human motion generation. We adopt the same metrics as previous works, including Frechet Inception Distance (FID) for motion quality, Retrieval Precision (R-Precision) and Multi-Modal Distance (MM-Dist) for text-motion consistency, and Diversity and MultiModality (MModality) for the diversity of generated motions. We denote two sets of features from the ground truth and generated motion as m and \hat{m} , respectively.

N	R-Precision \uparrow			FID \downarrow	MM-Dist \downarrow	Diversity \rightarrow
	Top-1	Top-2	Top-3			
Reconstruction						
1	0.493 \pm .002	0.681 \pm .002	0.787 \pm .003	0.170 \pm .001	3.160 \pm .015	9.589 \pm .074
3	0.501 \pm .002	0.696 \pm .002	0.792 \pm .004	0.117 \pm .000	3.037 \pm .007	9.621 \pm .091
5	0.508 \pm .003	0.700 \pm .003	0.795 \pm .002	0.080 \pm .000	3.004 \pm .008	9.620 \pm .098
7	0.513 \pm .002	0.704 \pm .003	0.797 \pm .002	0.022 \pm .000	2.984 \pm .009	9.603 \pm .085
Generation						
1	0.498 \pm .003	0.686 \pm .004	0.791 \pm .004	0.424 \pm .009	3.085 \pm .009	9.705 \pm .097
3	0.523 \pm .004	0.712 \pm .002	0.814 \pm .002	0.418 \pm .025	2.946 \pm .009	9.443 \pm .136
5	0.523 \pm .003	0.715 \pm .002	0.815 \pm .002	0.188 \pm .006	2.915 \pm .007	9.488 \pm .099
7	0.514 \pm .004	0.713 \pm .005	0.813 \pm .003	0.291 \pm .006	2.938 \pm .012	9.456 \pm .130

Table 8. Study on the number of latent vectors in motion VAE on the HumanML3D [19] test set.

γ_{attn}	γ_{reg}	Per-crop semantic correctness				Realism	
		R@1 \uparrow	R@3 \uparrow	TMR-Score \uparrow M2T	M2M	FID \downarrow	Transition distance \downarrow
0.0	0.0	12.7	25.4	0.570	0.562	0.592	2.7
0.1	0.2	1.4	4.2	0.498	0.495	1.083	6.1
0.01	0.02	9.1	20.1	0.551	0.547	0.623	2.9
0.005	0.01	6.7	15.3	0.531	0.523	0.806	1.9
0.005	0.005	13.8	25.6	0.570	0.558	0.591	2.7
0.001	0.002	14.0	26.3	0.570	0.560	0.587	2.7

Table 9. Ablation of step size in Adaptive Gradient Descent on MTT [47].

FID. The Fréchet Inception Distance (FID) measures the quality of generated motions by comparing their feature distributions to ground truth motions. It evaluates both the mean and covariance. Lower FID scores indicate better quality and closer resemblance to real data. FID can be calculated as:

$$\text{FID} = \|\mu_m - \mu_{\hat{m}}\|^2 - \text{TR}(\Sigma_m + \Sigma_{\hat{m}} - 2\Sigma_m \Sigma_{\hat{m}}) \quad (12)$$

where μ_{gt} and $\mu_{\hat{m}}$ are mean of two sets of features. Σ is the covariance matrix.

MM-Dist. MM-Dist is used to measure the distance between the generated motion and text directly:

$$\text{MM-Dist} = \frac{1}{N} \sum_{i=1}^N \|m_i - \hat{m}_i\| \quad (13)$$

where N is the total number of the motion.

Diversity. To assess the diversity among motions generated by different textual descriptions in the test set, we randomly select 300 pairs of motions and compute this metric

as follows:

$$\text{Diversity} = \frac{1}{300} \sum_{i=1}^{300} \|\hat{m}_1 - \hat{m}_2\| \quad (14)$$

MModality. Similar to **Diversity**, MModality is used to measure the diversity among motions generated by the same text. We follow Guo *et al.* [19] to generate 30 motion samples from one text and randomly select two subsets, each containing 10 motions. The formulation of MModality is similar to the **Diversity** described above.

For compositional motion generation, we follow STMC [47] to use R-Precision, TMR-Score, FID, and transition distance to evaluate the performance. Similar to MM-Dist, TMR-Score computes the cosine similarity between the generated motion embedding and text embedding with TMR model [46]. TEACH [2] calculates Euclidean distance between two consecutive frames as transition distance.

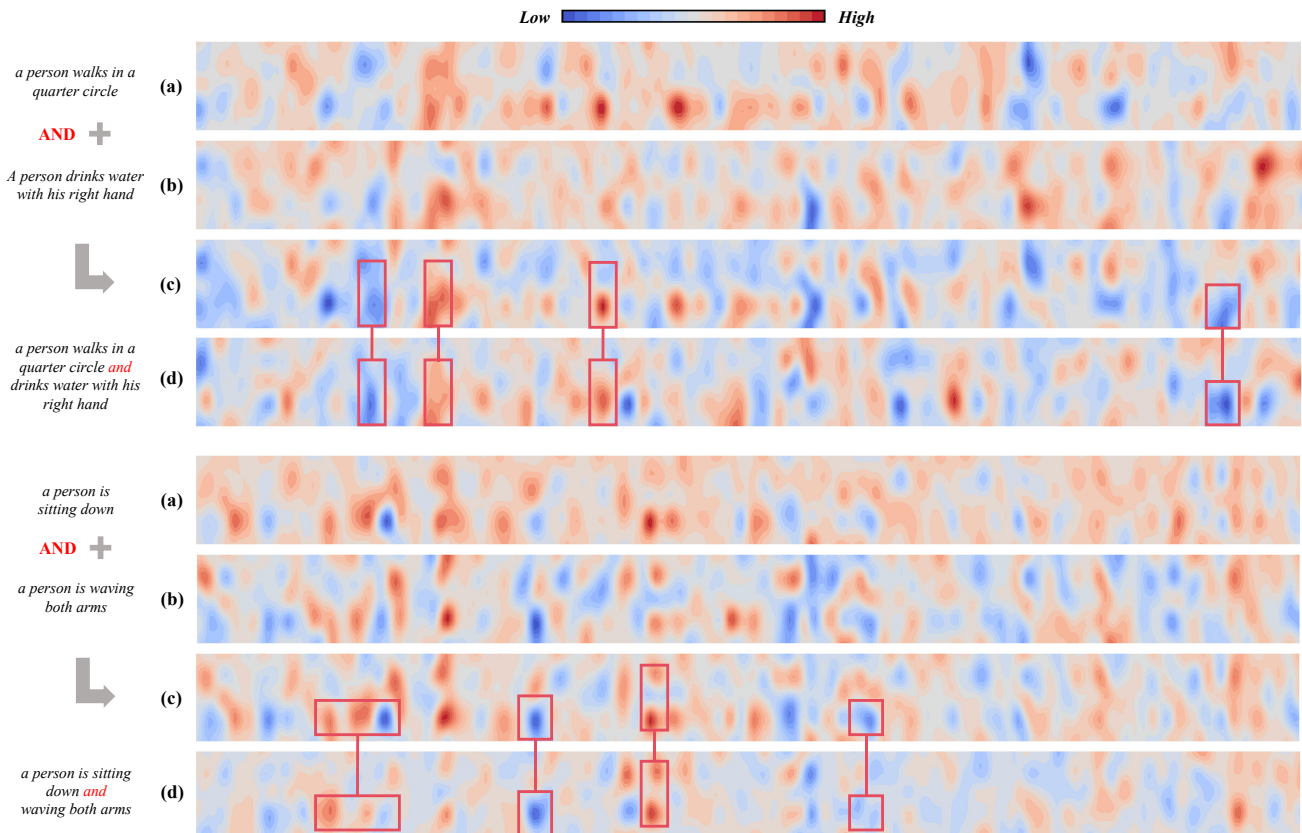


Figure 6. **Visual results of energy distributions.** For a clear illustration, energy distributions are calculated with interpolation and Gaussian smoothing and then visualized as contour maps. (a) Concept 1, (b) Concept 2, (c) Compositional motion generation, (d) Multi-concept motion generation. Similar regions are highlighted in red